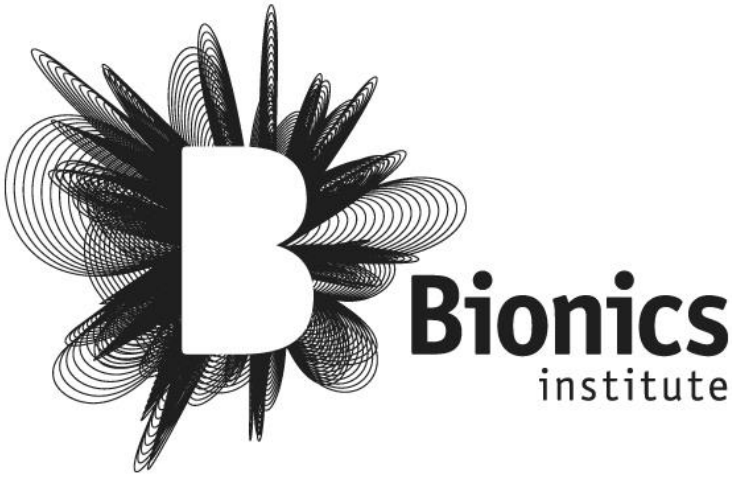

Title: An *in vivo* investigation of inferior colliculus single neuron responses to cochlear nucleus pulse train stimulation

Authors: Stefan J. Mauger[1,2,3], Mohit N. Shivdasani[1,2,3], Graeme D. Rathbone[2,3] & Antonio G. Paolini[1,2]

[1] School of Psychological Science, La Trobe University, VIC 3086, Australia

[2] Bionics Institute, East Melbourne, VIC 3002, Australia

[3] Department of Electronic Engineering, La Trobe University, VIC 3086, Australia

Running heading: Cochlear nucleus pulse train stimulation

Corresponding Author: Antonio Paolini, School of Psychological Sciences, La Trobe University, Victoria, Australia, 3086, a.paolini@latrobe.edu.au, +61 3 9479 2947

Abstract:

The auditory brainstem implant (ABI) is being used clinically to restore hearing to patients unable to benefit from a cochlear implant (CI). Speech perception outcomes for ABI users are typically poor compared to most CI users. The ABI is implanted either on the surface of, or penetrating through, the cochlear nucleus (CN) in the auditory brainstem, and utilizes stimulation strategies developed for auditory nerve stimulation with a CI. Although stimulus rate may affect speech perception outcomes with current stimulation strategies, no studies have systematically investigated the effect of stimulus rate electrophysiologically or clinically. We therefore investigated rate response properties and temporal response properties of single inferior colliculus (IC) neurons from penetrating ABI stimulation using stimulus rates ranging from 100 to 1600 pulses per second in the rat. We found that stimulus rate affected the proportion of response types, thresholds, and dynamic ranges of IC activation. Stimulus rate was also found to affect the temporal properties of IC responses, with higher rates providing more temporally similar responses to acoustic stimulation. Suppression of neural firing and inhibition in IC neurons was also found, with response properties varying with stimulus rate. This study has demonstrated that changes in ABI stimulus rate results in significant differences in IC neuron response properties. Due to electrophysiological differences, stimulus rate may also change perceptual properties. We suggest that clinical evaluation of ABI stimulus rate should be performed.

Keywords: Cochlear Nucleus, Auditory Brainstem Implant, Inferior Colliculus, Pulse Train Stimulation, Stimulus Rate, Electrical Stimulation

Introduction:

Auditory brainstem implants (ABIs) electrically stimulate the central auditory pathway at the level of the Cochlear Nucleus (CN) (Edgerton et al. 1982) to restore hearing. Although well over 800 recipients have received an ABI worldwide (Colletti et al. 2009b; Otto et al. 2002), speech perception by ABI users is typically poor compared to most cochlear implant (CI) users. (Briggs et al. 2000; Colletti et al. 2005; Colletti et al. 2009a; Colletti and Shannon 2005; Kanowitz et al. 2004; Nevison et al. 2002; Otto et al. 2002).

The CN is the first central auditory nucleus receiving input, and maintains tonotopicity from the cochlea through the auditory nerve (Rose et al. 1959). It contains multiple sub-divisions and neuron types that participate in parallel pathways of processing (Cant and Benson 2003). Each neuron type has unique anatomical and physiological properties, and is thought to code for specific acoustic features (Rhode and Smith 1986). Due to electrode size and placement of the ABI, stimulation of the CN usually results in broad fields of neural activation. This may cause activation of multiple neuron populations, and probably activation of multiple parallel ascending pathways.

In CI recipients, the stimulus rate providing best speech perception outcomes and general rate preference is typically user specific, ranging between 250 and 1800 pps (Arora et al. 2011; Vandali et al. 2000). A clinical study of three auditory midbrain implant (AMI) recipients found that a stimulus rate of 250 pps was most suitable, with lower rates resulting in unwanted rate-pitch effects and higher rates resulting in rapid loudness adaptation (Lim et al. 2009; Lim et al. 2008). The historical, and still the predominant, stimulus rate used in ABIs is approximately 250 Hz (Colletti et al. 2009b; McCreery 2008; Otto et al. 2002; Schwartz et al. 2008). Clinical studies using higher stimulus rates have suggested that this may result in improved speech perception (Behr et al. 2007; Colletti 2006; Colletti et al. 2005), possibly due

71 to increased temporal resolution (Colletti et al. 2005; Colletti et al. 2009b) or improved
72 activation of specific neuron types (McCreery 2008). The systematic investigation of the effect
73 of ABI stimulation rate has not been performed electrophysiologically or perceptually. Such
74 results may lead to improved speech performance outcomes for ABI users.
75
76 The aim of this study was to investigate neural firing rate and temporal response properties of
77 single IC neurons from penetrating ABI stimulation at a range of clinically relevant stimulus
78 rates. Electrical stimulation of the CN with different stimulus rates may elicit a range of
79 complex firing rate and temporal responses in the IC, due to multiple cell types and parallel
80 pathways of processing between the CN and IC. A further aim of this study was to investigate
81 if inhibitory neural pathways between these structures are activated through ABI stimulation.
82
83

Materials and Methods:

Surgery and Electrode Implantation

Experiments were performed on male Hooded Wistar rats (n=15) weighing between 265 and 410gms (Flinders University, SA, Australia) and anaesthetized with urethane (intraperitoneally, 20% wt/vol in dH_2O; Sigma-Aldrich, Castle Hill, NSW, Australia). Recordings were performed in a sound attenuating Faraday room on a gas anti-vibration table (Technical Manufacturing Corporation, Peabody, MA). Animals were mounted in a stereotaxic frame with ear bars (David Kopf Instruments, Tujunga, CA), and their temperature maintained at 37°C. A section of the cerebellum was aspirated to aid electrode placement in the left CN. A multichannel electrode array (Neuronexus Technologies, Ann Arbor, MI) was implanted using a microcontroller into the ventral cochlear nucleus (VCN) at an approximate 30 degree caudo-rostral angle. VCN electrodes consisted of four shanks spaced 200 μm apart with eight 413 μm^2 iridium-oxide electrode sites spaced 200 μm apart on each shank. Electrode activation was performed prior to implantation (Anderson et al. 1989), lowering electrode impedances to approximately 90 kΩ at 1 kHz.

After VCN probe placement, tones ranging from 10 dB to 60 dB sound pressure level (SPL) (10 dB SPL steps) and 1 kHz to 60 kHz (1/4 octave steps below 4 kHz and 1/7 octave steps above 4 kHz) were presented (20 repetitions) to determine the response area and characteristic frequency (CF; frequency that produced the highest response rate at the lowest acoustic intensity) of each electrode site. All tones were 50 ms in duration with 5 ms rise and fall times and a 500 ms inter-trial interval.

Single neurons in the contralateral Central Nucleus of the Inferior Colliculus (CIC) were recorded from using quartz glass microelectrodes filled with 1M potassium acetate solution. Electrodes were advanced through the CIC at an approximate 15 degree rostro-caudal angle.

When a single CIC neuron was isolated, an approximate best frequency (BF; frequency that produced the highest response rate at a given acoustic intensity) was found at 60 dB SPL by manually varying the tone frequency. An automatic protocol was then initiated that presented acoustic tones at 60 dB SPL over a three octave bandwidth, with five repetitions per $1/7^{th}$ octave frequency increment, with the neuron's approximate BF in the centre of this range. Recordings in the CIC were verified through a gradual increase in BF in a dorso-ventral direction (Merzenich and Reid 1974), and no habituation of response to acoustic stimulation (Spitzer and Semple 1993). All procedures were carried out in accordance with St Vincent's Hospital animal ethics committee guidelines.

CN Electrical Stimulation and CIC Recordings

Following IC responses to acoustic stimulation, electrical stimuli were presented to electrode sites in the VCN that had similar CFs to the BF of the CIC neuron. Pulse trains of varying stimulus rates were presented for the first 50 ms of each 500 ms repetition. Pulse train stimulus rates of 100, 200, 400, 800 and 1600 pulses per second (pps) were used. Five repetitions of the same stimulus parameters were presented at 12 to 15 current levels ranging from 0 to 40 μA. Single pulse stimuli were additionally presented for neurons where intracellular recordings were achieved. In these cases, a single pulse at the start of each 500 ms repetition was presented at the same current levels used for pulse train stimulation. All electrical pulses were cathodic-leading biphasic pulses of 120 μs per phase with a 40 μs interphase gap. For CIC neurons that responded with short time-locked latencies indicative of antidromic activation, a collision test was performed (Bishop et al. 1962; Darian-Smith et al. 1963). Antidromic behavior was confirmed by presenting an acoustic click stimulus, resulting in a CIC spike, which caused the abolition of a subsequent spike produced from delayed CN stimulation (Mauger et al. 2010). Common ground stimulation was employed with one stimulation site, and the surrounding electrode sites as returns. This type of stimulation was selected as it has been

shown to provide more place-specific activation than monopolar stimulation (Cicione et al. 2012).

Artifact Removal

Artifacts in IC extracellular recordings were approximately ten times the amplitude of action potentials. Signal processing techniques were employed to suppress artifacts while maintaining spikes in recordings. Response traces were imported to Matlab (The Mathworks, Natika, MA) and processed with custom-made programs. Five responses to the same parameter set were high-pass filtered to remove DC components and normalized so each repetition had the same RMS power during the stimulus period. The median of the five traces was then subtracted from each trace individually, enabling action potentials to be located (Litvak et al. 2001). For intracellular recordings, signal processing was used to maintain low frequency intracellular recording content such as excitatory post synaptic potentials, and particularly inhibitory post synaptic potentials. For pulse rates of 400 pps and above, a low pass Butterworth filter was used to suppress high frequency artifacts. The remaining artifact was removed using a moving average filter with a temporal length of the stimulus period. For pulse rates of 100 and 200 pps a technique was used where samples just before and just after stimulation were interpolated between to remove artifacts (O'Keeffe et al. 2001).

Data Analysis

A second custom Matlab program was then used that located action potentials for both acoustically and electrically evoked CIC responses. All response traces were visually checked as some spikes were not found through the automatic method. This ensured that all spikes were included in the analysis, particularly traces with the same stimulus parameters that exhibited very little variability in spike latency from each other. In the small number of such cases, the accuracy of visually locating spikes was not different from the automatic method.

Thresholds at each stimulus rate were determined as the lowest current level that produced a firing rate, in the first 70 ms post stimulus onset, higher than the mean plus two standard deviations of the spontaneous firing rate (calculated from 90 ms to 300 ms post stimulus onset). Where the spontaneous firing rate was less than one spike per repetition, threshold was determined as the current level that produced at least one spike per repetition in the first 70 ms of the stimulus.

Rate-level functions of CIC neurons from VCN electrical stimulation at each stimulus rate were categorized into four groups (Fig. 1A), previously defined by acoustic stimulation experiments (Aitkin and Schuck 1985). Rate-level functions exhibiting an increasing firing rate with increasing current level were classified as monotonic. Rate-level functions where firing rate increased with current level but then remained constant or decreased slightly, but not below 50% of the maximum firing rate were classified as plateau. Rate-level functions where firing rate increased, but then decreased below 50% of the maximum firing rate were classified as non-monotonic. A fourth group of rate-level functions that did not fit into any of the first three categories were classified as complex. For monotonic responses, saturation was calculated as the maximum current level used. For plateau responses, a sigmoid curve was fitted to the rate-level function, and the current level at 90% of the asymptote of the sigmoid was used as the neuron's saturation. For both non-monotonic and complex neural responses, the current level that produced the maximum firing rate was taken as the CIC neuron's saturation. Thresholds and saturation current levels were used to calculate dynamic ranges.

Results:

Data from 33 CIC neurons were collected, of which 24 were extracellular recordings and 9 were intracellular recordings. Extracellularly recorded neurons were included in the database where BFs were found and where VCN stimulation using at least one stimulus rate was performed at all current levels. Of these neurons, 14 (58%) responded to at least one stimulus rate, four showed suppression in neural firing, two showed antidromic behavior and four showed no response to electrical stimulation. Detailed analysis on the effect of pulse rate on neural responses was performed on the 14 responsive CIC neurons. Analysis of CIC neurons whose spontaneous action potentials were suppressed by electrical stimulation was also performed. Of the nine intracellularly recorded neurons, five were recorded in response to single pulse stimulation and four were recorded in response to both single pulse and pulse train stimulation of the VCN.

CIC Rate-level Functions

Analysis of rate-level functions found 8% of the neurons exhibited a monotonic response to 100 pps, while for stimulus rates greater than 400 pps, approximately 35% of responses were monotonic. Plateau responses were the most common when using a stimulus rate of 1600 pps. The highest proportion of non-monotonic responses was seen with 200 pps, followed by 400 pps, while 800 pps showed almost 50% complex responses. A decreasing trend in non-responses was found with increased stimulus rate (Fig. 1B). It should also be noted that electrical stimulation did not activate four of the recorded neurons at any stimulus rate.

Thresholds and Dynamic Ranges

Thresholds in the CIC from electrical stimulation ranged between 2 and 40 μA. Some variance was seen between neurons, with many neurons having thresholds decreasing to 2 μA at higher stimulus rates (Fig. 2A). For statistical analysis, neurons that did not reach threshold by the

maximum current level (40 μA) were given the maximum as their threshold. A one-way repeated measures analysis of variance (ANOVA) on thresholds showed a significant main effect of stimulus rate ($F(4,38)=6.00$, $p<0.001$). Newman-Keuls *post hoc* comparisons found significant decreases in thresholds from 100 pps to all other stimulus rates (200 pps ($p<0.05$), 400 pps ($p<0.01$) and 800 pps ($p<0.01$) and 1600 pps ($p<0.05$)).

Dynamic ranges in the CIC from electrical stimulation ranged from 0 to 26 dB (Fig. 2B). Much variance in dynamic range across stimulus rates was seen. In the analysis of dynamic range, a repeated measures ANOVA found no significant main effect of stimulus rate ($F(4,30)=1.77$, $p=0.162$). This could be in part due to missing data points from neurons not reaching threshold.

Neural Firing Rate

CIC neuron firing rates of less than five spikes per repetition in response to VCN electrical stimulation were common (Fig. 2C), however firing rates of up to 19 spikes per repetition were found for some neurons. In the analysis of firing rate, a repeated measures ANOVA showed a significant main effect of stimulus rate ($F(4,38)=5.265$, $p<0.001$). Newman-Keuls *post hoc* comparisons did not show significant differences between stimulus rates.

Vector Strength and Inter Spike Interval

A measure of the degree of phase locking (vector strength) to individual electrical stimuli was calculated for each CIC neuron. A similar method previously used for phase locking to acoustic stimuli was implemented (Goldberg and Brown 1969; Greenwood and Durand 1955; Johnson 1980), where the time point of each spike, i, was considered defining a vector of unit length with the phase angle θ_i (equation 1).

$$\theta_i = \frac{2\pi \times spike\ time_i}{stimulus\ period} \quad (1)$$

The n vectors, characterizing spike trains at the saturation current for each neuron at each stimulus rate, were used to calculate vector strength (equation 2).

$$Vector\ Strength = \frac{\sqrt{(\sum \sin\theta_i)^2 + (\sum \cos\theta_i)^2}}{n} \quad (2)$$

For stimulus rates of 100 and 200 pps, vector strengths as high as 0.98 were seen, while for stimulus rates greater than 400 pps a maximum vector strength of 0.6 was seen (Fig. 2D). The effect of rate on mean vector strength across all neurons was analyzed with a repeated measures ANOVA and was found to be not significant ($F(4,15)=0.639$, $p=0.643$).

Temporal Response Comparison

To investigate the stimulus rate that produced a neural response with temporal characteristics most similar to those produced by acoustic stimulation, peri-stimulus time histograms (PSTHs) were constructed using 10 ms bins (Fig. 3A, C). Each PSTH was normalized so the sum of all bins was 1. Normalized PSTHs were averaged across all neurons for both acoustic stimulation (Fig. 3B) and electrical stimulation (Fig. 3D). In response to acoustic stimulation, CIC neurons typically responded with a peak in neural firing between 10 and 20 ms after stimulus onset, with a decreasing response after this period. In response to electrical stimulation using stimulus rates of 100 and 200 pps, neurons tended to show more consistent firing rates over the duration of the stimulus. At stimulus rates of 800 and 1600 pps, responses peaked between 10 and 20 ms, and gradually decreased thereafter (Fig. 3D), similar to acoustic stimulation. Differences between PSTHs elicited by acoustic and electrical stimulation are shown in Figure 3E, with mean differences shown in Figure 3F. A rate of 800 pps produced the lowest average difference in firing rates between acoustic and electrical stimulation (Fig. 3F).

To further compare temporal responses, correlation coefficients between acoustic and electrical PSTHs were calculated for all stimulus rates (Fig. 3G). Stimulus rates of 100 and 200 pps were poorly correlated to acoustic stimulation while stimulation rates of 400 pps and above gave

correlation coefficients as high as 0.9 (Fig. 3H). A one-way ANOVA found a significant change in correlation coefficient across stimulus rate ($F(4,27)=3.07$, $p<0.05$).

Suppression of spontaneous firing

Of the total 24 neurons recorded extracellularly, four (17%) neurons showed suppression in neural firing to electrical stimulation. An example of the typical suppression pattern is shown as a raster plot in Figure 4A for a single neuron at stimulus rates of 100, 400 and 1600 pps. Suppression of spontaneous activity increased in duration in a monotonic fashion with an increase in current level for all four neurons. Stimulus rates of 100 pps produced long lasting suppression, up to 50 ms after stimulus cessation. Higher stimulus rates were found to produce shorter suppression periods. Excitation was also seen at low current levels (8 to 15 μA) using 400 pps and 1600 pps (Fig. 4B). This excitation was not seen at higher current levels. Neural firing post suppression tended to recommence at similar times for traces at the same current level. Spontaneous activity had a period of approximately 50 ms.

Intracellular Responses

Intracellular recordings of nine CIC neurons to VCN electrical stimulation were analyzed to see the effects of excitation and inhibition. Responses of four neurons were recorded to both single-pulse and pulse train VCN stimulation. Responses of two intracellularly recorded neurons to acoustic and electrical stimulation at a range of stimulus rates are shown in Figures 5 and 6. Acoustic responses showed early onset inhibition (Fig. 5A) or no inhibition (Fig. 6A), characterized by the presence of inhibitory post synaptic potentials. At low stimulus rates, inhibition from each stimulus pulse was found, which resulted in strong inhibition for the duration of the electrical stimulation (Fig. 5B, 6B). At higher stimulus rates inhibitory responses became more complex, with the length of inhibition shorter than the stimulus duration (Fig. 5B, 6B). Action potentials, after cessation of the stimulus at low rates and

directly after the cessation of inhibition at higher rates, were also found (Fig. 6B). Both inhibition depth (Fig. 5C, 6C) and inhibition duration (Fig. 5D, 6D) were measured across current level for each stimulus rate. Inhibition depth was found to increase relatively linearly with current level for each stimulus rate. Higher stimulus rates had comparatively lower inhibition levels across current levels. Inhibition duration for 100 pps and 200 pps lasted the whole stimulation duration for current levels above threshold. A more gradual increase in inhibition duration was found for 400 pps and 800 pps (Fig. 5D, 6D). In the case of 800 pps, the duration of the inhibition seemed to plateau at approximately 22 ms for moderate to high current levels.

Intracellular responses to single pulse stimulation at a number of VCN electrode sites with similar CFs to the BF of the CIC neuron were analyzed (Fig. 7). Strong inhibition after electrical stimulation was seen from stimulation of all electrode sites (Fig. 7A). Inhibition depth was found to increase with current levels, but at different rates for different stimulating electrodes (Fig. 7B). Electrodes located closer to the Octopus cell region (ventro-caudal) showed stronger inhibition in CIC neuron 9-1 but little difference was seen for CIC neuron 13-3 (Fig. 7C).

Discussion:

Excitatory Responses

Unlike CIC responses from auditory nerve stimulation where rate-level functions are predominantly monotonic (and plateau), and less commonly non-monotonic (Semple and Kitzes 1985; Shepherd et al. 1999), a fourth response type was observed in this study. These complex rate-level responses have also been reported in a previous VCN electrical stimulation study (Shivdasani et al. 2008). High stimulation rates produced a higher proportion of monotonic and plateau responses and the least number of non-responses. However, an increase of complex response patterns was also found at higher rates. Lower average thresholds and higher firing rates were expected from higher stimulus rates due to increased total current, but could also be as a result of increased excitability, or decreased inhibition from higher stimulus rates.

The temporal arrangement of spikes is thought to contain information from many acoustic features, including amplitude, frequency and source location (Furukawa and Middlebrooks 2002; Heil 2004; Moore 2003). We therefore compared temporal spike arrangement in the CIC in response to VCN electrical stimulation. Higher electrical stimulus rates produced responses with lower vector strength (increased stocasticity), which in a stimulation strategy is thought to desynchronize the fiber population and may improve temporal resolution and dynamic range (Rubinstein et al. 1999). A comparison of PSTHs in response to acoustic and electrical stimulation showed that high stimulus rates better represented acoustic temporal firing patterns in CIC neurons from stimulation of central VCN regions. It is possible that higher stimulus rates may also provide benefit to ABI users compared to the present clinical stimulus rate of 250 pps. A number of papers have suggested that higher stimulus rates may lead to improved speech perception (Behr et al. 2007; Colletti 2006; Colletti et al. 2005). More recently, a consortium of data has shown that using stimulus rates above 1200 pps can result in significant

speech improvement results compared to rates below 1200 pps ($p<0.027$) in ABI patients (Shannon 2012). But as stimulus rate also affected clinical thresholds, and pulse widths were not consistent across stimulus rate, the effect of rate alone could not be definitively stated.

Inhibitory Responses

Although VCN neuron populations providing inhibitory input to the CIC are well described, there has been very little discussion on the effects of activating these pathways through VCN electrical stimulation. Extracellular recordings showing suppression of neural firing and intracellular recordings showing inhibitory post synaptic potentials (IPSPs) in this study have been able to demonstrate electrical activation of ascending inhibitory pathways. This could be through activation of Octopus cells that respond to signal onsets (Hemmert et al. 2005), providing fast inhibition to the CIC through the Ventral Nucleus of the Lateral Lemniscus (Nayagam et al. 2005). Another possibility could be through GABA-ergic intrinsic connections within the CIC itself (Adams and Mugnaini 1984; Faingold et al. 1991). Similar long lasting suppression of spontaneous firing, such as seen in our extracellular recordings at low stimulus rates, has also been described in response to acoustic stimulation, although the origin of such inhibition is unknown (Carney and Yin 1989). A previous VCN electrical stimulation study showed that two VCN electrodes 'when stimulated individually' were able to elicit CIC responses, however, when stimulated together it was possible to abolish the CIC response (Shivdasani et al. 2010), suggesting complex interactions between excitation and inhibition. Although the inhibitory pathway is important and well described for acoustic stimulation, the effects of inhibition from ABI stimulation are unclear. A systematic study to investigate the effect of increased or decreased activation of the inhibitory pathway from ABI stimulation would help in determining its contribution and importance.

Suppression seen in extracellular recordings and the presence of IPSPs in our intracellular recordings were highly dependent on the stimulus rate used. Low electrical stimulation rates were found to provide more suppression of firing, while higher rates provided shorter durations of suppression. Similarly, for low stimulus rates, inhibition was seen to last longer than the stimulation duration and had increased depth, while at higher stimulus rates both the depth and duration of inhibition decreased. Location of stimulation was also found to affect inhibition depth. An increase in inhibition from stimulation of more ventral and caudal VCN electrodes was observed, possibly due to their proximity to the Octopus cell region. It is possible that the reduction of inhibition at higher stimulus rates, particularly at 800 pps, might be attributed to the band-pass characteristics of Octopus cells, shown to have an upper band limit of approximately 650 Hz (Godfrey et al. 1975; Hemmert et al. 2005).

Clinical Translation

Similarities between mammalian auditory systems have enabled the extensive use of rats and cats in auditory research (Adams 1986; Moore 1987; Moore and Osen 1979), however, some differences would influence implications of our results for humans. The human VCN contains relatively fewer Octopus neurons than the rat VCN. If the inhibition seen in our recordings is through the Octopus cell pathway, then the effect of activating these pathways through CN stimulation may be decreased in humans. Another significant difference is the much larger granule cell domain in humans that contains GABA-ergic small cells. The projections of such neurons are predominantly to the fusiform cells in the dorsal CN (Mugnaini et al. 1980), which in turn project to the CIC (Berrebi and Mugnaini 1991). Our study was conducted with the auditory nerve intact. ABI recipients typically do not have a functioning auditory nerve, and therefore it is accepted that responses may differ due to plastic changes. In many NF2 cases, the auditory nerve would at least be partially functioning before tumor removal, resulting in a short deafness period and possibly minimal long term deafness changes in neural re-organization. It

may be important to investigate how plasticity due to auditory nerve removal affects responses to VCN electrical stimulation. The use of anaesthesia may also influence our experimental findings, and needs to be considered when comparing to awake function.

Implications for ABIs

Current ABIs use vocoder stimulation strategies developed for CIs that aim to vary the level of activation of frequency specific neural populations through current level. This study has shown that stimulus rate has a range of effects on CIC neural response properties. A clinical ABI study on stimulus rate should be carried out to determine if significant psychoacoustic changes or changes in speech perception outcomes are also found at higher rates.

One study has suggested that specific cell types such as T-stellate neurons, thought to carry frequency information to the CIC, may be important to activate by ABIs (McCreery 2008). Although neuron groups in the VCN are unable to be stimulated separately, being intermingled with, or in close proximity to other neuron groups, it may be possible to target specific neural populations by varying stimulus rate. Such targeted stimulation is supported by the different depolarization patterns between cell types such as T-stellate and Octopus neurons (Ferragamo and Oertel 2002). Selection of a stimulus rate that activates a desired neuron type over other neuron types in proximity may be possible, either continuously, or dynamically.

Electrode location in this study was also suggested to affect the level of inhibition. The clinical penetrating auditory brainstem implant (PABI) was designed to target cell populations in the central VCN similar to the regions activated in this study. Unfortunately there has been no significant improvement in speech perception results from PABI recipients compared to ABI users (Otto et al. 2008). The PABI, with its surface and penetrating electrodes, would be well suited to assessing perception from both electrode location and stimulus rate.

Conclusion

This study systematically investigated rate response properties, temporal response properties and inhibition in the IC from CN electrical stimulation. Higher stimulus rates produced lower thresholds and more similar temporal responses to acoustic stimulation compared to lower stimulus rates. Strong inhibition was found from electrical stimulation, with stimulus rate found to affect the depth and duration of inhibition. These complex inhibitory and excitatory results may have implications for the development of future ABI stimulation strategies. Additional electrophysiological testing is required to further explore the effect of electrode placement on inhibition. Due to many differences in IC response properties seen across stimulus rate, clinical testing with ABI and PABI recipients with a range of stimulus rates, particularly high rates, may lead to improved outcomes.

Acknowledgements: We thank Dr Conor Hogan from the Department of Chemistry, La Trobe University, for assistance with preparing our stimulating electrodes. We also thank Rebecca Argent for histological and animal assistance and Courtney Suhr for animal assistance. We also would like to thank three unnamed reviewers who provided significant comments resulting in an improved manuscript.

Grants: Funding was provided by the Garnett Passe and Rodney Williams Memorial Foundation. The Bionic Ear Institute acknowledges the support it receives from the Victorian Government through its Operational Infrastructure Support Program.

Figure 1. ***A****, Examples of rate responses to a range of current levels. Solid black lines show rate-level functions, dashed lines show 50% of maximum firing rate, gray lines shows spontaneous firing rate.* ***B****, Percentage of neurons at a range of stimulus rates grouped by response type. Stimulus rate is shown in increasing order with the first (left) bar in each group representing 100 pps (n=14), 200 pps (n=13), 400 pps (n=12), 800 pps (n=11) and the last (right) bar representing 1600 pps (n=6).*

***Figure 2. A**, Absolute thresholds of CIC neurons at a range of stimulus rates. Each line represents data from a single neuron. A significant decrease in threshold was seen across stimulus rate (* denotes p<0.05, ** denotes p<0.01). **B**, Dynamic range (dB) of neurons plotted against stimulus rate. **C**, Individual lines showing maximum firing rate at any current level plotted against stimulus rate. **D**, Vector strength plotted against stimulus rate for each IC neuron.*

Figure 3. ***A****, Individual lines show proportion of spikes falling in the first 70 ms after the start of acoustic stimulation for each IC neuron.* ***B****, Mean acoustic PSTH for all neurons showing a moderate onset response followed by a decrease in activation towards the end of stimulation.* ***C****, Individual lines show proportion of spikes falling after the start of electrical stimulation for each neuron at a range of current levels for different stimulus rates.* ***D****, Mean electrical PSTH for all stimulus rates.* ***E****, Difference between acoustic and electrical PSTHs (acoustic minus electrical) for each neuron.* ***F****, Mean difference between acoustic and electrical PSTHs for all stimulus rates.* ***G****, Correlation coefficient between each neuron's acoustic and electrical PSTH at each stimulus rate.* ***H****, Average correlation coefficients for each stimulus rate. All PSTH were computed using 10 ms bin width.*

Figure 4. *Analysis of a single IC neuron to a range of electrical stimulation rates.* ***A****, Raster plots of spike locations across time for all current levels. Electrical stimuli were presented for the first 50 ms, and examples are shown for stimulus rates of 100 pps, 400 pps and 1600 pps. For each current level, five repetitions are overlaid. A black bar along the abscissa shows the duration of electrical stimulation. For low stimulus rates a low threshold, long lasting suppression of spontaneous firing activity was found.* ***B****, Combined PSTHs for four current levels between 8 and 15 μA and for four current levels between 28 and 40 μA inclusive. In each PSTH, data is displayed from 20 stimulus repetitions. For the period after 100 ms the average inter-spike interval is approximately 50 ms for all stimulus rates and current levels.*

Figure 5. ***A***, *Intracellular responses of IC neuron 9-1 (five traces overlaid) to acoustic stimulation at the neuron's best frequency showing initial inhibition followed by excitation.* ***B***, *Mean responses to electrical stimulation of neuron 9-1 at 40 μA (black) and 20 μA (gray).* ***C***, *Plot of the depth of inhibition across current level. Each symbol type represents a different stimulus rate. Linear trend lines through each stimulus rate are also shown. A drop in inhibition depth can be seen for 800 pps compared to lower rates.* ***D***, *Plot of the duration of inhibition across current level. Symbols represent the same rate as in subplot C. A decrease in the inhibition duration can be seen for 400 pps compared to lower rates, and for 800 pps compared to 400 pps.*

Figure 6. ***A****, Intracellular responses of neuron 13-3 (five traces overlaid) to acoustic stimulation at the neuron's best frequency showing excitation.* ***B****, Mean responses to electrical stimulation of neuron 13-3 at 40 µA (black) and 20 µA (gray).* ***C****, Plot of the depth of inhibition across current level. Each symbol type represents a different stimulus rate. Linear trend lines through each stimulus rate are also shown. A drop in inhibition depth can be seen for 400 pps and 800 pps compared to lower rates.* ***D****, Plot of the duration of inhibition across current level. Symbols representing the same stimulus rates as in subplot C. A decrease in the inhibition duration can be seen for 400 pps compared to lower rates, and for 800 pps compared to 400 pps.*

***Figure 7. A**, Mean responses of CIC neuron 9-1 (top), and neuron 13-3 (bottom) at 40 μA to single pulse stimulation across a number of VCN electrode sites. Artifact can be seen at stimulus onset, followed by different levels of inhibition. Symbols on the top right of each graph correspond to the symbols in subplot C, which denote VCN electrode location. Closed symbols represent sites stimulated while recording from neuron 9-1 and open symbols represent sites stimulated while recording from neuron 13-3 in all subplots. **B**, Plot of the depth of inhibition across current level for three different VCN electrode sites for CIC neuron 9-1 and neuron 13-3. A much larger variance in inhibition depths can be seen for neuron 9-1 than for neuron 13-3. **C**, A diagrammatical representation of a VCN electrode, showing the locations of stimulating electrode sites on the electrode array. Electrodes consisted of 4 shanks, and 8 electrode sites on each shank. Symbols correspond to electrode locations stimulated while recording from neuron 9-1 (filled) and neuron 13-3 (open). The direction of the Octopus cell region is also shown.*

References:

Adams JC. Neuronal morphology in the human cochlear nucleus. *Arch Otolaryngol Head Neck Surg* 112: 1253-1261, 1986.

Adams JC and Mugnaini E. Dorsal nucleus of the lateral lemniscus: a nucleus of GABAergic projection neurons. *Brain Res Bull* 13: 585-590, 1984.

Aitkin L and Schuck D. Low frequency neurons in the lateral central nucleus of the cat inferior colliculus receive their input predominantly from the medial superior olive. *Hear Res* 17: 87-93, 1985.

Anderson DJ, Najafi K, Tanghe SJ, Evans DA, Levy KL, Hetke JF, Xue XL, Zappia JJ, and Wise KD. Batch-fabricated thin-film electrodes for stimulation of the central auditory system. *IEEE Trans Biomed Eng* 36: 693-704, 1989.

Arora K, Vandali A, Dowell R, and Dawson P. Effects of stimulation rate on modulation detection and speech recognition by cochlear implant users. *Int J Audiol* 50: 123-132, 2011.

Behr R, Muller J, Shehata-Dieler W, Schlake HP, Helms J, Roosen K, Klug N, Holper B, and Lorens A. The High Rate CIS Auditory Brainstem Implant for Restoration of Hearing in NF-2 Patients. *Skull Base* 17: 91-107, 2007.

Berrebi AS and Mugnaini E. Distribution and targets of the cartwheel cell axon in the dorsal cochlear nucleus of the guinea pig. *Anat Embryol (Berl)* 183: 427-454, 1991.

Bishop PO, Burke W, and Davis R. Single-unit recording from antidromically activated optic radiation neurones. *J Physiol* 162: 432-450, 1962.

Briggs RJ, Fagan P, Atlas M, Kaye AH, Sheehy J, Hollow R, Shaw S, and Clark GM. Multichannel auditory brainstem implantation: the Australian experience. *J Laryngol Otol Suppl*: 46-49, 2000.

Cant NB and Benson CG. Parallel auditory pathways: projection patterns of the different neuronal populations in the dorsal and ventral cochlear nuclei. *Brain Res Bull* 60: 457-474, 2003.

Carney LH and Yin TC. Responses of low-frequency cells in the inferior colliculus to interaural time differences of clicks: excitatory and inhibitory components. *J Neurophysiol* 62: 144-161, 1989.

Cicione R, Shivdasani MN, Fallon JB, Luu CD, Allen PJ, Rathbone GD, Shepherd RK, and Williams CE. Visual cortex responses to suprachoroidal electrical stimulation of the retina: effects of electrode return configuration. *J Neural Eng* 9: 036009, 2012.

Colletti V. Auditory outcomes in tumor vs. nontumor patients fitted with auditory brainstem implants. *Adv Otorhinolaryngol* 64: 167-185, 2006.

Colletti V, Carner M, Miorelli V, Guida M, Colletti L, and Fiorino F. Auditory brainstem implant (ABI): new frontiers in adults and children. *Otolaryngol Head Neck Surg* 133: 126-138, 2005.

Colletti V, Shannon R, Carner M, Veronese S, and Colletti L. Outcomes in nontumor adults fitted with the auditory brainstem implant: 10 years' experience. *Otol Neurotol* 30: 614-618, 2009a.

Colletti V and Shannon RV. Open set speech perception with auditory brainstem implant? *Laryngoscope* 115: 1974-1978, 2005.

Colletti V, Shannon RV, Carner M, Veronese S, and Colletti L. Progress in restoration of hearing with the auditory brainstem implant. *Prog Brain Res* 175: 333-345, 2009b.

Darian-Smith I, Phillips G, and Ryan RD. Functional Organization in the Trigeminal Main Sensory and Rostral Spinal Nuclei of the Cat. *J Physiol* 168: 129-146, 1963.

Edgerton BJ, House WF, and Hitselberger W. Hearing by cochlear nucleus stimulation in humans. *Ann Otol Rhinol Laryngol Suppl* 91: 117-124, 1982.

Faingold CL, Boersma Anderson CA, and Caspary DM. Involvement of GABA in acoustically-evoked inhibition in inferior colliculus neurons. *Hear Res* 52: 201-216, 1991.

Ferragamo MJ and Oertel D. Octopus cells of the mammalian ventral cochlear nucleus sense the rate of depolarization. *J Neurophysiol* 87: 2262-2270, 2002.
Furukawa S and Middlebrooks JC. Cortical representation of auditory space: information-bearing features of spike patterns. *J Neurophysiol* 87: 1749-1762, 2002.
Godfrey DA, Kiang NY, and Norris BE. Single unit activity in the posteroventral cochlear nucleus of the cat. *J Comp Neurol* 162: 247-268, 1975.
Goldberg JM and Brown PB. Response of binaural neurons of dog superior olivary complex to dichotic tonal stimuli: some physiological mechanisms of sound localization. *J Neurophysiol* 32: 613-636, 1969.
Greenwood J and Durand D. The distribution of length and components of the sim of *n* random unit vectors. *Ann Math Stats*: 233-246, 1955.
Heil P. First-spike latency of auditory neurons revisited. *Curr Opin Neurobiol* 14: 461-467, 2004.
Hemmert W, Holmberg M, and Ramacher U. Temporal sound processing by cochlear nucleus neurons. *Lecture Notes in Computer Science* 3696: 583-588, 2005.
Johnson DH. The relationship between spike rate and synchrony in responses of auditory-nerve fibers to single tones. *J Acoust Soc Am* 68: 1115-1122, 1980.
Kanowitz SJ, Shapiro WH, Golfinos JG, Cohen NL, and Roland JT, Jr. Auditory brainstem implantation in patients with neurofibromatosis type 2. *Laryngoscope* 114: 2135-2146, 2004.
Lim HH, Lenarz M, and Lenarz T. Auditory midbrain implant: a review. *Trends Amplif* 13: 149-180, 2009.
Lim HH, Lenarz T, Joseph G, Battmer RD, Patrick JF, and Lenarz M. Effects of phase duration and pulse rate on loudness and pitch percepts in the first auditory midbrain implant patients: Comparison to cochlear implant and auditory brainstem implant results. *Neuroscience* 154: 370-380, 2008.
Litvak L, Delgutte B, and Eddington D. Auditory nerve fiber responses to electric stimulation: modulated and unmodulated pulse trains. *J Acoust Soc Am* 110: 368-379, 2001.
Mauger SJ, Shivdasani MN, Rathbone GD, Argent RE, and Paolini AG. An in vivo investigation of first spike latencies in the inferior colliculus in response to multichannel penetrating auditory brainstem implant stimulation. *J Neural Eng* 7: 036004, 2010.
McCreery DB. Cochlear nucleus auditory prostheses. *Hear Res* 242: 64-73, 2008.
Merzenich MM and Reid MD. Representation of the cochlea within the inferior colliculus of the cat. *Brain Res* 77: 397-415, 1974.
Moore BC. Coding of sounds in the auditory system and its relevance to signal processing and coding in cochlear implants. *Otol Neurotol* 24: 243-254, 2003.
Moore JK. The human auditory brain stem: a comparative view. *Hear Res* 29: 1-32, 1987.
Moore JK and Osen KK. The cochlear nuclei in man. *Am J Anat* 154: 393-418, 1979.
Mugnaini E, Warr WB, and Osen KK. Distribution and light microscopic features of granule cells in the cochlear nuclei of cat, rat, and mouse. *J Comp Neurol* 191: 581-606, 1980.
Nayagam DA, Clarey JC, and Paolini AG. Powerful, onset inhibition in the ventral nucleus of the lateral lemniscus. *J Neurophysiol* 94: 1651-1654, 2005.
Nevison B, Laszig R, Sollmann WP, Lenarz T, Sterkers O, Ramsden R, Fraysse B, Manrique M, Rask-Andersen H, Garcia-Ibanez E, Colletti V, and von Wallenberg E. Results from a European clinical investigation of the Nucleus multichannel auditory brainstem implant. *Ear Hear* 23: 170-183, 2002.
O'Keeffe DT, Lyons GM, Donnelly AE, and Byrne CA. Stimulus artifact removal using a software-based two-stage peak detection algorithm. *J Neurosci Methods* 109: 137-145, 2001.
Otto SR, Brackmann DE, Hitselberger WE, Shannon RV, and Kuchta J. Multichannel auditory brainstem implant: update on performance in 61 patients. *J Neurosurg* 96: 1063-1071, 2002.

606 **Otto SR, Shannon RV, Wilkinson EP, Hitselberger WE, McCreery DB, Moore JK, and**
607 **Brackmann DE**. Audiologic outcomes with the penetrating electrode auditory brainstem
608 implant. *Otol Neurotol* 29: 1147-1154, 2008.
609 **Rhode WS and Smith PH**. Encoding timing and intensity in the ventral cochlear nucleus of
610 the cat. *J Neurophysiol* 56: 261-286, 1986.
611 **Rose JE, Galambos R, and Hughes JR**. Microelectrode studies of the cochlear nuclei of the
612 cat. *Bull Johns Hopkins Hosp* 104: 211-251, 1959.
613 **Rubinstein JT, Wilson BS, Finley CC, and Abbas PJ**. Pseudospontaneous activity:
614 stochastic independence of auditory nerve fibers with electrical stimulation. *Hear Res* 127:
615 108-118, 1999.
616 **Schwartz MS, Otto SR, Shannon RV, Hitselberger WE, and Brackmann DE**. Auditory
617 brainstem implants. *Neurotherapeutics* 5: 128-136, 2008.
618 **Semple MN and Kitzes LM**. Single-unit responses in the inferior colliculus: different
619 consequences of contralateral and ipsilateral auditory stimulation. *J Neurophysiol* 53: 1467-
620 1482, 1985.
621 **Shannon R**. Keynote Panel Discussion - Auditory brainstem implantations: Considerations for
622 improved results. *International Conference on Cochlear Implants & Other Implantable*
623 *Technologies*, edited by Niparko JK, Baltimore, Maryland USA, 2012.
624 **Shepherd RK, Baxi JH, and Hardie NA**. Response of inferior colliculus neurons to electrical
625 stimulation of the auditory nerve in neonatally deafened cats. *J Neurophysiol* 82: 1363-1380,
626 1999.
627 **Shivdasani MN, Mauger SJ, Argent RE, Rathbone GD, and Paolini AG**. Inferior colliculus
628 responses to dual-site intralamina stimulation in the ventral cochlear nucleus. *J Comp Neurol*
629 518: 4226-4242, 2010.
630 **Shivdasani MN, Mauger SJ, Rathbone GD, and Paolini AG**. Inferior colliculus responses to
631 multichannel microstimulation of the ventral cochlear nucleus: implications for auditory brain
632 stem implants. *J Neurophysiol* 99: 1-13, 2008.
633 **Spitzer MW and Semple MN**. Responses of inferior colliculus neurons to time-varying
634 interaural phase disparity: effects of shifting the locus of virtual motion. *J Neurophysiol* 69:
635 1245-1263, 1993.
636 **Vandali AE, Whitford LA, Plant KL, and Clark GM**. Speech perception as a function of
637 electrical stimulation rate: using the Nucleus 24 cochlear implant system. *Ear Hear* 21: 608-
638 624, 2000.
639

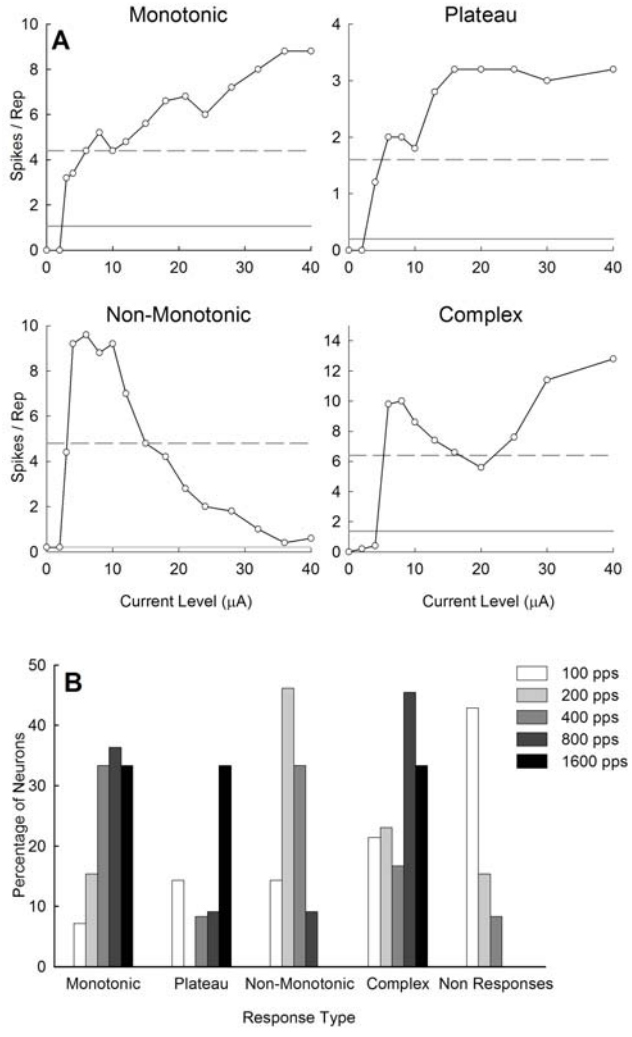
A
Monotonic
Plateau
Non-Monotonic
Complex
Spikes / Rep
Current Level (μA)
B
100 pps
200 pps
400 pps
800 pps
1600 pps
Percentage of Neurons
Monotonic
Plateau
Non-Monotonic
Complex
Non Responses
Response Type

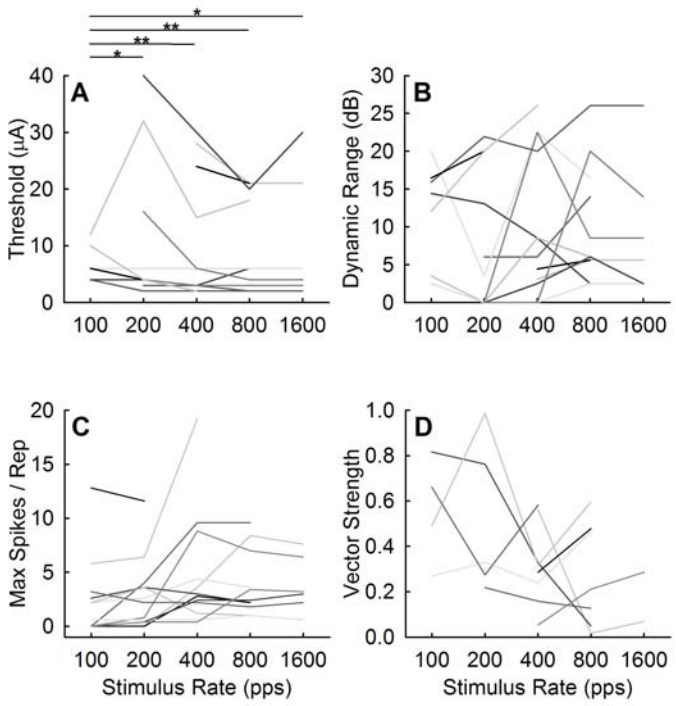
*
**
**
*
A
Threshold (μA)
40
30
20
10
0
100 200 400 800 1600
B
Dynamic Range (dB)
30
25
20
15
10
5
0
100 200 400 800 1600
C
Max Spikes / Rep
20
15
10
5
0
100 200 400 800 1600
Stimulus Rate (pps)
D
Vector Strength
1.0
0.8
0.6
0.4
0.2
0.0
100 200 400 800 1600
Stimulus Rate (pps)

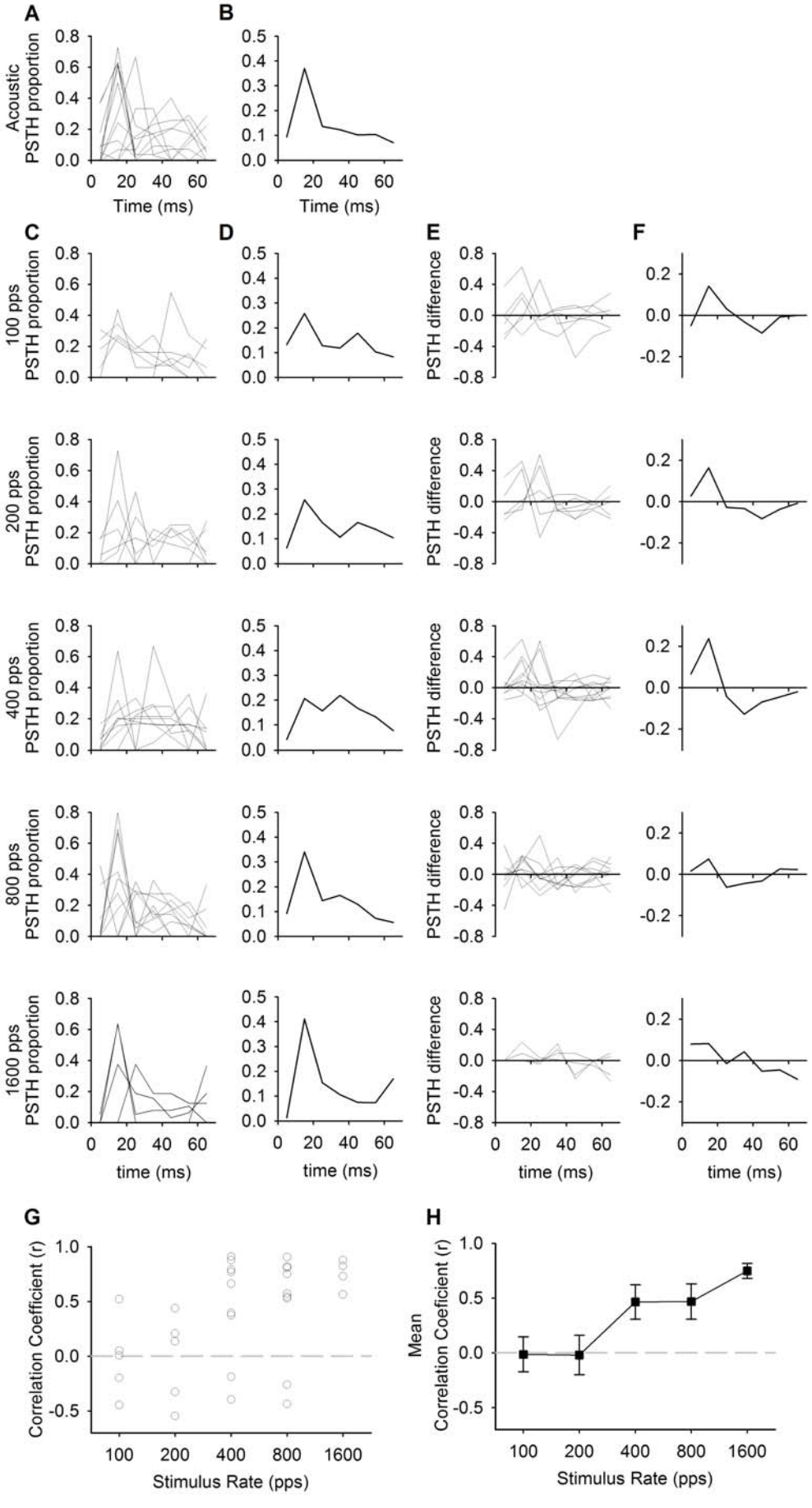
A
B
C
D
E
F
G
H
Acoustic PSTH proportion
100 pps PSTH proportion
200 pps PSTH proportion
400 pps PSTH proportion
800 pps PSTH proportion
1600 pps PSTH proportion
PSTH difference
Time (ms)
time (ms)
Correlation Coefficient (r)
Mean Correlation Coeficient (r)
Stimulus Rate (pps)
100
200
400
800
1600

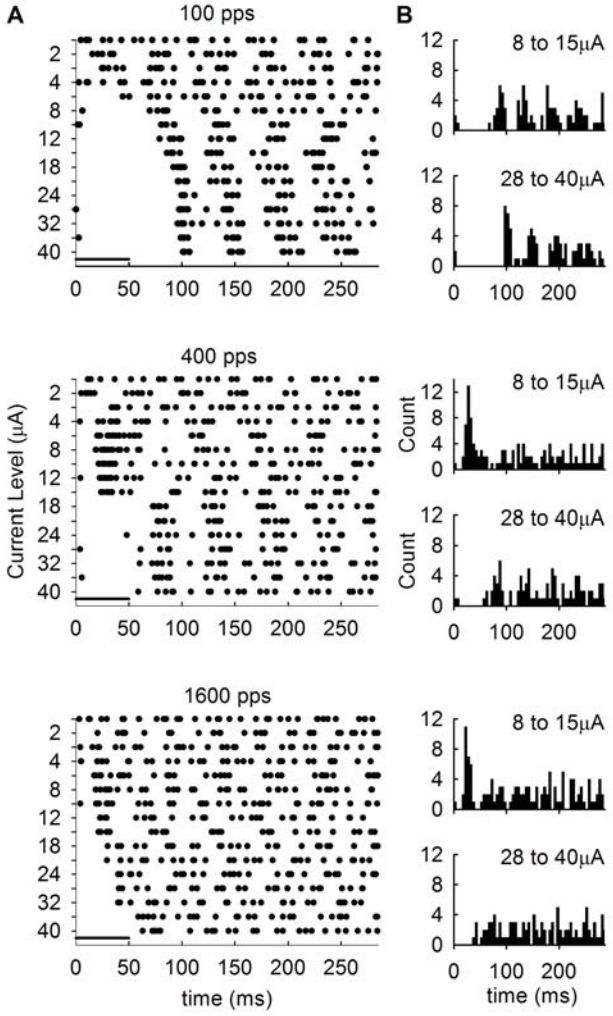
A
B
100 pps
400 pps
1600 pps
Current Level (μA)
2
4
8
12
18
24
32
40
0
50
100
150
200
250
time (ms)
8 to 15μA
28 to 40μA
Count
12
8
4
0
100
200

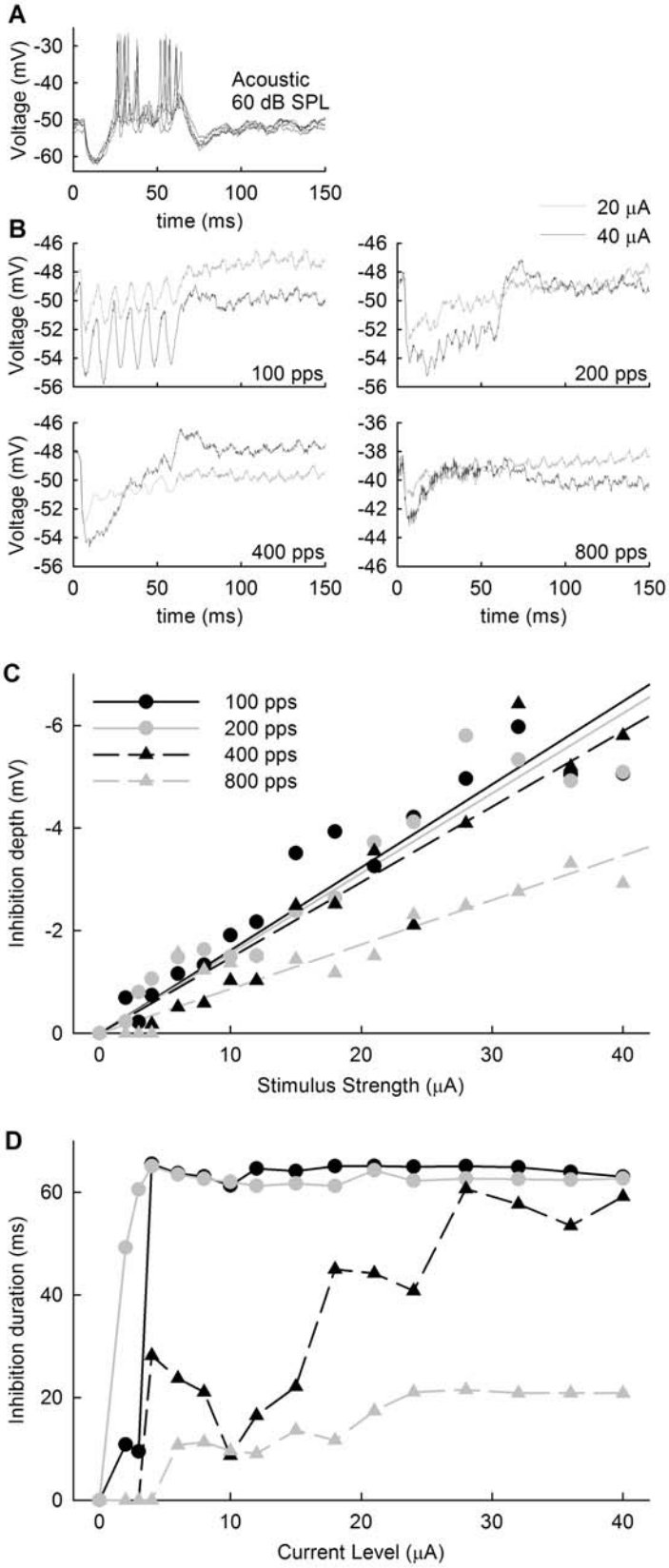
A
Voltage (mV)
-30
-40
-50
-60
Acoustic
60 dB SPL
0
50
100
150
time (ms)
B
20 μA
40 μA
Voltage (mV)
-46
-48
-50
-52
-54
-56
100 pps
200 pps
-36
-38
-40
-42
-44
400 pps
800 pps
time (ms)
C
100 pps
200 pps
400 pps
800 pps
Inhibition depth (mV)
-6
-4
-2
0
10
20
30
40
Stimulus Strength (μA)
D
Inhibition duration (ms)
60
40
20
Current Level (μA)

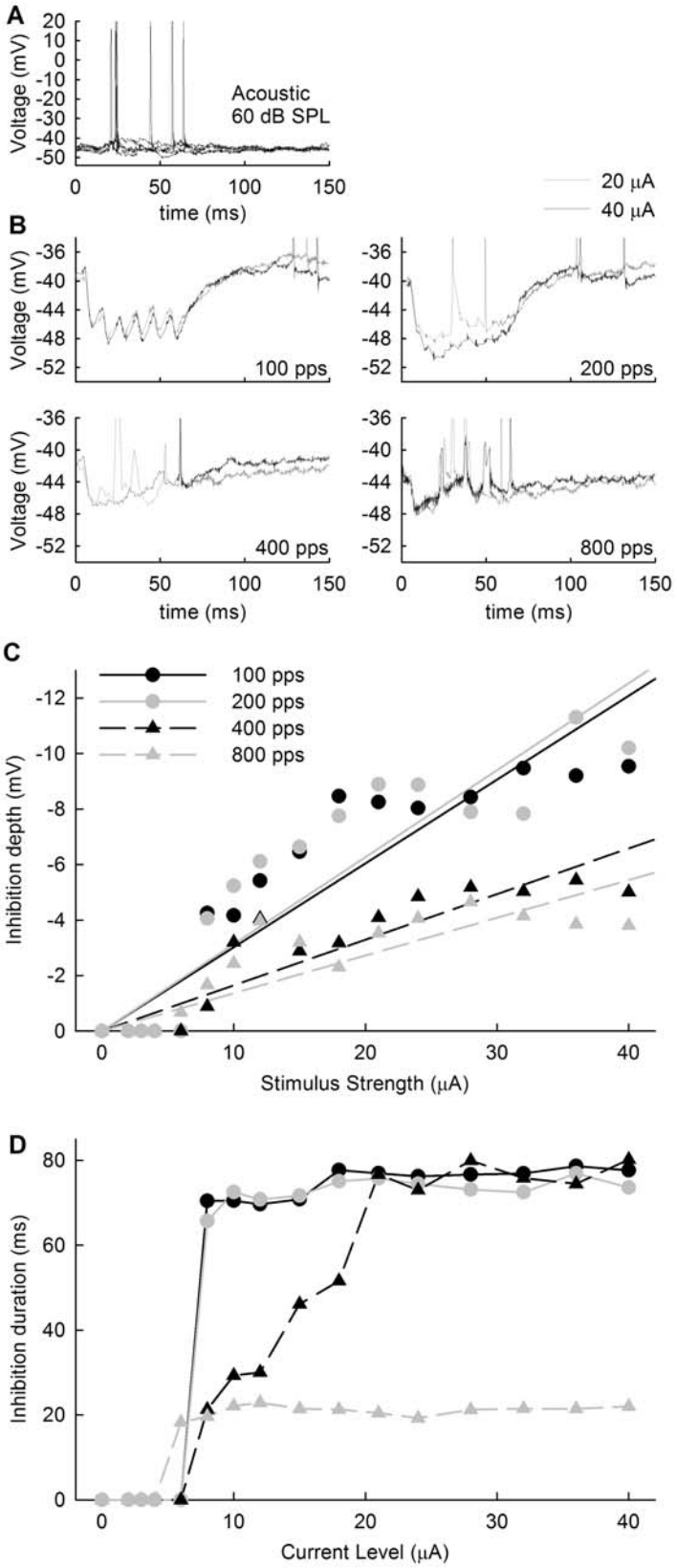
A
Voltage (mV)
Acoustic
60 dB SPL
time (ms)
B
20 μA
40 μA
100 pps
200 pps
400 pps
800 pps
C
Inhibition depth (mV)
Stimulus Strength (μA)
D
Inhibition duration (ms)
Current Level (μA)

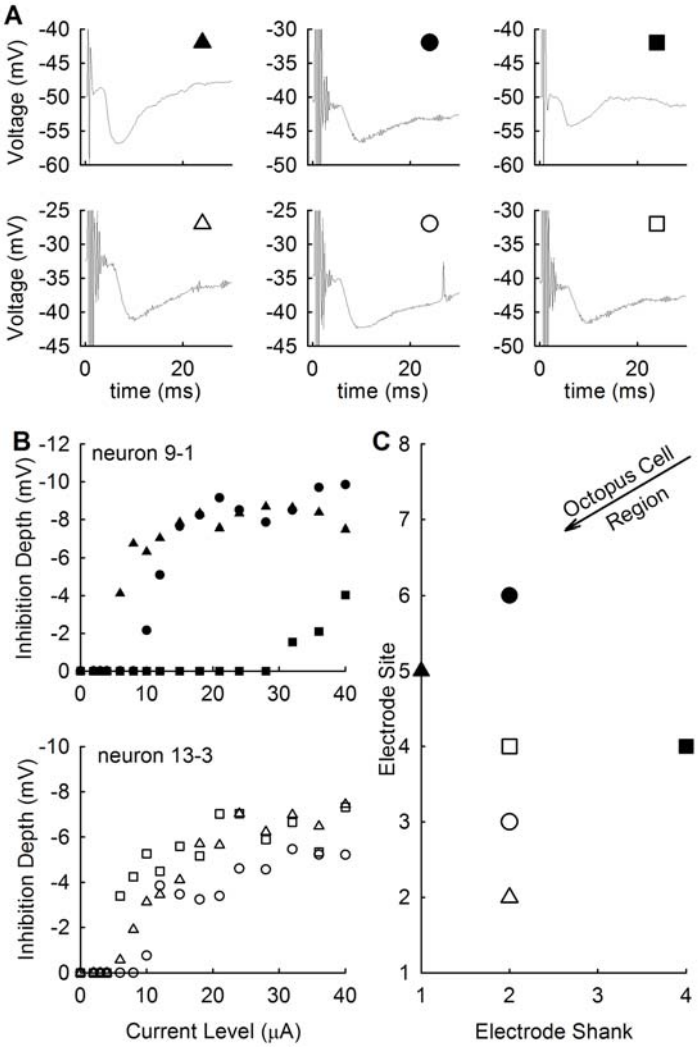
A
Voltage (mV)
time (ms)
B
neuron 9-1
neuron 13-3
Inhibition Depth (mV)
Current Level (μA)
C
Octopus Cell Region
Electrode Site
Electrode Shank